Air-and-N_2 broadening parameters of HDO and D_2O; 709 to 1936 cm^{-1}

Robert A. Toth

California Institute of Technology

Jet Propulsion Laboratory

Pasadena California 91109

e-mail: toth@caesar.jpl.nasa.gov

Tables 4

Figures 6

ABSTRACT

High resolution measurements of air and N_2 broadened widths and pressure-induced frequency-shifts of HDO and D_2O covering the spectral region between 700 and 2000 cm^{-1} were obtained with absorption paths of 2.39m, 25m, 73m, and 193m. The majority of the measurements included the (010)-(000) bands of $HD^{16}O$ and $D_2{}^{16}O$. Also measured were 17 lines of the pure rotational band of $HD^{16}O$ and several transitions of the (010)-(000) bands of $HD^{18}O$ and $D_2{}^{18}O$ and a few transitions of the "hot" band, (020)-(010), for $HD^{16}O$ and $D_2{}^{16}O$. The observed width coefficients ranged from 0.02 to 0.1 cm^{-1}/atm. and the pressure-induced shift coefficients fell between +0.012 to -.012 cm^{-1}/atm. Line mixing was observed for a few of the pairs of transitions of HDO but was of no consequences for D_2O lines. However the effects of line mixing were small and accurate results were obtained using the Voigt line profile. Collisional narrowing effects were not observed in the data.

1. INTRODUCTION

In two recent studies (1,2), low pressure measurements were obtained for HDO(1) and D_2O(2) of which the data provided accurate values for line positions and strengths for an extensive coverage of the (010)-(000) bands of $HD^{16}O$ and $D_2{}^{16}O$ as well as first time measurements and assignments of the (000)-(000) band of $HD^{16}O$ above 600 cm^{-1}. Also reported for the first time were measurements of the "hot" bands, (020)-(010) and (100)-(010) for $HD^{16}O$ and the triad: (020)-(010), (100)-(010), and (001)-(010) of $D_2{}^{16}O$. Results from those investigations(1,2) along with prior studies(3,4) form an accurate representation of line positions (low pressure) and strengths for all of the transitions of $HD^{16}O$, $HD^{17}O$, $HD^{18}O$, $D_2{}^{16}O$, $D_2{}^{17}O$, and $D_2{}^{18}O$ which appear in the experimental data used in the present work.

The present study compliments two previous investigations by Rinsland et al.(5,6) who reported broadening and shift coefficients for HDO broadened by N_2, air, and O_2(5) and comparable parameters for D_2O(6) also broadened by these buffer gases. They(5,6) obtained their data using the same instrument that was used in this work and covered the stronger transitions of HDO and D_2O with an absorption path length of 1.21m for both experiments. The absorption path lengths used to obtain the data here were 2.4m, 25m, 73m, and 193m with buffer gases of N_2 and dry air. The experimental conditions for the spectral runs are listed in Table 1.

2. EXPERIMENT

The laboratory spectra were recorded with a Fourier transform spectrometer (FTS) located in the McMath Solar Telescope facility at the Kitt Peak National Observatory. The IR radiation from a globar source was collected onto a liquid He-cooled arsenic-doped silicon single element detector. Sample temperatures were inferred from thermistor probes in thermal contact with the absorption cell walls. Sample pressures were measured with a Baratron gauge with a ten (combined HDO, D_2O, and H_2O pressures) and 1000 (total sample pressure) Torr pressure heads. The 1000 Torr head was calibrated against room air pressure (~600 Torr) which was measured separately with a high accuracy mercury manometer. The FTS runs each consisted of 12 or more interferograms co-added over a period of an hour or more to achieve a signal-to noise ratio of 200:1 or better. The composite interferograms were transformed into spectral data at the Kitt Peak facility and then transferred via computer to JPL.

The experimental conditions given in table 1 list the spectral coverage of the measurements, the unapodized spectral resolution, the absorption path lengths, sample pressures, and percent abundances of the three water vapor species. Spectral runs with path lengths of 25m or longer were obtained with a 6m base length multiple transversal absorption cell. The optical path from the 6m cell to the vacuum tank, which enclosed the FTS, was about 5.4m and contained the 2.39m long glass cell (used for the N_2-broadened runs) and compartments which were purged with dry N_2. This configuration greatly reduced interference from spectral

absorptions due to normal amounts of CO_2, N_2O, CH_4, and mainly $H_2{}^{16}O$ contained in the room air.

The vacuum tank which enclosed the FTS was continuously evacuated with a diffusion pump however a very small amount (~200 μm pressure) of residue room air was never removed. Spectral runs made with the globar source placed directly in front of the vacuum tank entrance showed narrow, spectral features due to the strongest absorption lines of H_2O and CO_2 (600-700 cm^{-1}). As expected, these lines were also observed in spectral runs obtained with the 2.39m long cell as well as the 6m cell evacuated. Evacuated cell runs (not given in Table 1) were made directly before and after the other sets of runs listed in the table and they served the purpose as frequency calibration runs using H_2O line positions given by Toth(7) and CO_2 frequencies listed in the HITRAN(8) compilation.

The last five entries given in Table 1 show that the gas samples were H_2O from which the strongest HDO spectral lines were measured. The other entries in the table were of runs in which the gas samples were a mixture of $HDO/D_2O/H_2O$. The gas samples were prepared from a mixture of liquid H_2O with D_2O with more D_2O than H_2O in the contents in order to minimize the contributions due to broadened H_2O. In any event, the mixtures allowed the HDO portion of the samples to be almost one-half of the total gas sample amounts.

3.DATA ANALYSIS

The analysis of the spectra was done by the same method as

that used in a similar study of air- and N_2-broadening parameters of H_2O covering the same spectral region(9). The method is based upon a non-linear least-squares (NLLS) fitting technique in which the input list consisted of an accurate representation of the line positions and strengths of the observed lines and also a good knowledge of the linewidth parameters for these transitions. For this purpose, the input list consisted of the parameters derived from low sample pressure studies of H_2O(7,10), HDO(1,3) and D_2O(2,4) along with broadening parameters given in high foreign pressure studies of H_2O(9), HDO(5), and D_2O(6). The pressure broadening parameters for many of the HDO and D_2O lines observed in the present data were not known or given with low accuracy from those studies(5,6). Therefore, prior to using the NLLS program, a preliminary analysis was performed in order to obtain a more accurate parameter listing for input to the fitting program.

Using the NLLS program, the line positions, strengths and widths of the observed lines were fitted along with other parameters (continuum, slope, and 100% transmission level) in an interactive mode on the computer. The computer program took into account the spectral resolution convoluted with line profile algorithms which consisted of Doppler to Voigt line shape representations. Other inputs to the NLLS program included the absorbing gas pressures, buffer gas pressures, and path lengths. The preliminary analysis also served as a "gauge" to determine accurate values of the absorbing gas pressures. The procedure for filling an absorption cell was as follows. The absorbing gases

were initially entered into the cell and measured and, after a period of time, the foreign gas was let into the cell and the total pressure measured. Due to residue water vapor adsorbed into the cell walls before the foreign gas was entered(9) and since the absorbing gas consisted of three species of water vapor, accurate values of the partial pressures of HDO and D_2O, given in Table 1, were determined from spectral analysis using line strength values given in refs. (1-4). Due to room air in the empty space between the source and vacuum tank, the H_2O content in the absorption cell was not derived from spectral analysis. Instead, the H_2O partial pressure, for a given run, was derived from the difference between the low pressure Baratron gauge reading and the sum of the HDO and D_2O partial pressures (obtained from spectral analysis). The low pressure values obtained from pressure gauge readings gave somewhat less than an accurate account of the sum of the three partial gas pressures after the foreign gas was entered. Tests made with H_2O broadened by air spectra indicate that the low pressure readings (H_2O) may be off by 5%-20% following the above mentioned experimental procedure. A study of the entries given in Table 1, excluding the bottom five, which were runs used in my recent study(9), show that an uncertainty of 20% in the low pressure reading translates to less than 0.2% uncertainty in the foreign gas pressure value. The foreign gas pressure values given in table 1 were derived from the expression:

$$P(f) = P(T) - P(L), \qquad (1)$$

where f, T, and L mean foreign, total, and low pressures, respectively. For spectral analysis using the NLLS program, the H_2O content used in the derivation of the input list was adjusted to account for the optical density of H_2O in the open space between source and vacuum tank. The open space H_2O optical density was ~4.4 m-Torr when the 6m absorption cell was used. The 2.39m long cell was placed directly in front of the entrance to the vacuum tank so that minimal contributions due to room air were observed in those spectra.

4. LINE MIXING

Line mixing effects occur in the broadening of several molecules. Most notable is the effect on the Q-branch transitions of the 15 μm ground state band of CO_2 of which corrections to the Voigt line profile are stated and given in the HITRAN(8) study. Only recently have these effects been observed in water vapor absorptions. Brown and Plymate(11) observed but did not report this effect on two pairs of of $H_2{}^{16}O$ transitions broadened by H_2. The pairs involve the same rotational quantum numbers, J K_a K_c: one set is 3 0 3 ← 2 1 2 and 2 1 2 ← 1 0 1, and the other set is 1 0 1 ← 2 1 2 and 2 1 2 ← 3 0 3. The effect was also observed and reported by this author(9) for the same sets of transitions when the broadening agents were air and N_2, however the effect was about three times less than observed in the H_2-broadened data. These effects were found in the present set of air and N_2-broadened spectra for a few HDO lines but were not detected in any D_2O+air or

D_2O+N_2 spectral features.

Line mixing effects appear when the interacting pair of transitions are located close to each other and for the case of the two H_2O sets, the differences in line frequencies were 0.87 cm^{-1} and 1.3 cm^{-1}. The differences in line frequencies for the identical rotational transition pairs (given above) for $HD^{16}O$ is 11.068 cm^{-1} and 11.261 cm^{-1} and these values for $D_2{}^{16}O$ are 2.534 cm^{-1} and 2.621 cm^{-1}, however line mixing effects were not observed in the data for these rotational transitions for either species which may be due to their relatively large differences in frequencies.

Examples of closely spaced pairs of lines not affected by line mixing that were fitted accurately using the NLLS program are shown in Figures 1 and 2. Fig. 1 is a display of two $D_2{}^{16}O$ lines of the (010)-(000) band broadened by air: the rotational transitions, 5 4 2 ← 6 3 3 and 2 2 0 ← 3 1 3 located at 1182.470 cm^{-1} and 1182.803 cm^{-1}, respectively. The figure shows the % residuals between the observed and synthetic spectra located above the spectral plots. Fig 2. displays two other $D_2{}^{16}O$ lines with comparable rotational transitions: 11 6 6 ← 12 7 5 and 11 6 5 ← 12 7 6 located at 957.830cm^{-1} and 958.049 cm^{-1}, respectively.

Figures 3 and 4 show pairs of $HD^{16}O$ transitions of the (010)-(000) band that were affected by line mixing. The effect of line mixing is most evident in the figures by noting the differences between observed and synthetic spectra in the trough region between the interacting pairs. Figure 3 includes the pair of comparable

rotational transitions, 7 4 4 ← 8 5 3 and 7 4 3 ← 8 5 4 located at 1176.383 cm^{-1} and 1176.679 cm^{-1}, respectively, and Figure 4 involves another set of comparable transitions: 9 6 3 ← 9 5 4 and 9 6 4 ← 9 5 5, located at 1630.660 cm^{-1} and 1630.760 cm^{-1}, respectively. A study of the plots displayed in Figures 3 and 4 shows that the effects, due to air-broadening (as well as N_2-broadening), on the lines were not great and the results obtained using the Voigt profile differ by no more than 2% from a method using a more accurate line profile algorithm. Results from the NLLS fitting routine indicate that line mixing effects were very small or not evident for other HDO pairs of closely spaced lines of comparable transitions.

5. PARAMETER ANALYSIS

The measured line widths (HWHM), b, broadened by a foreign agent can be expressed in terms of the self- and foreign-broadening coefficients, b°_s and b°_f by:

$$b = P(f)b^\circ_f + P(s)b^\circ_s, \qquad (2)$$

where P(f) and P(s) are the foreign and self partial pressures. Values for b°_s were not derived in this study however self-broadened widths of H_2O were determined by Toth et al.(12). A calculation using those values(12) along with air-broadened widths of H_2O(9) show that the ratio of b°_s to b°_{air} for a H_2O transition is about 4.6, on the average, and this value was adopted for this study.

With this in mind, eq. (2) can be expressed as:

$$b = b^{\circ}_{f}[P(f) + 4.6P(s)], \qquad (3)$$

for air-broadened half-widths and close to this expression for N_2-broadened widths. The self partial pressure used in eqs. (2,3) represent the sum of the partial pressures of the three water vapor species. An uncertainty of 50% in b°_{s} or $b^{\circ}_{s}=(4.6\pm2.3)b^{\circ}_{f}$ results in an uncertainty in b°_{f} of 2% or less (less than 1% considering all runs) using eq. (3) and the experimental conditions given in Table 1.

The line shift parameters were not corrected for self-broadening effects. The expression used in this study was:

$$d = P(f)d^{\circ}_{f}, \qquad (4)$$

where d is the difference between the observed line position and the zero pressure line frequency and d°_{f} represents the pressure-induced frequency shift coefficient due to the buffer gas.

It was shown in refs.(9,12) that the half-width coefficients for H_2O can be ordered in terms of "families" of transitions. Within a "family" of transitions, the rotational quantum numbers obey the following rules: ΔJ, ΔK_a, K_a" ,γ', and γ" are the same and γ is defined as:

$$\gamma = K_a + K_c - J, \qquad (5)$$

and prime and double prime denote upper and lower states, respectively. As was done in the other studies(9,12) and also done here, smoothed values of linewidth coefficients, $b^{o}(sm)$, were derived from the experimental values from plots of "families" of rotational transitions. It was also stated in the other studies(9,12) that in the majority of cases, b^{o}_{f} or b^{o}_{s} for the rotational transitions, $J(n)K_{a}(n)K_{c}(n) \leftrightarrow J(m)K_{a}(m)K_{c}(m)$ have the same or nearly the same values and this was termed rotational reversal. The two sets of plots displayed in Fig. 5 illustrate the width behavior for transition pairs with their rotational quanta reversed (rotational reversal). The figure gives experimental values of b^{o}(air) for HDO P- and R-branch transitions plotted in terms of the lower state J value for the P-branch and the upper state J for the R-branch or in terms of $|m|$. The family types of transitions are shown in the upper portion of the figure. The data are presented in the figure without experimental uncertainties and without the smoothed values in order to lessen the confusion of the plots and therefore make it easier to see the match between respective P- and R-branch transitions whose quanta are reversed. Each plot shows a situation in which rotational reversal was not obeyed and they are displayed in the figure with a dashed oval containing the values of b^{o}(air).

The ordering of measurements of d^{o}_{f} in terms of "families" was found to be difficult and the concept of rotational reversal was rarely obeyed. In many cases, if d^{o}_{f} had a positive value for a given transition, then d^{o}_{f} was negative for the reversed rotational

transition. This was also the situation found in the H_2O broadening studies(9,12). By this token, smoothed values of $d°_f$ were not derived in this study however smoothed values of d°(air) were attempted and presented in my recent work(9).

Two examples of plots of d°(air) for D_2O are shown in Figure 6 displayed in a form similar to that of Figure 5. Inspection of the figure shows that the d°'s appear at random for any set of transitions (family of transitions) and that the concept of rotational reversal, for the most part, is not obeyed. The estimated uncertainties in the d°'s are not represented in Figure 6. In many cases, the uncertainties for $d°_f$ for HDO and D_2O were found to be large: up to 100% of the magnitude of $d°_f$.

6.RESULTS

The extensive listings of measured and computed line positions and strengths of the ν_2 bands were not given in my recent reports on $HD^{16}O$(1) and $D_2{}^{16}O$(2). These data were obtained at low sample pressures and path lengths up to and including 433m. Table 2 is an excerpt of the listing of the line position and strength parameters obtained in the recent study(1) along with linewidth and pressure-induced coefficients from the present work for the (010)-(000) band of $HD^{16}O$. The complete listing can be obtained from the author by e-mail. The computed positions given in the table represent the frequencies without the influence of pressure effects and were calculated from the energy levels given in ref. (1) and the uncertainty in the computed position, un, were derived from the

estimated uncertainties associated with energy level values. Line strength values listed were taken from ref. (1) and include the observed strength, the estimated uncertainty in the observed strength, %s, and the percent difference between the observed and computed strength, (o-c)%. Results from the present study follow in the table and include the air-broadening parameters, b°(sm), b°(obs), and d°(obs), followed by the same parameters for N_2-broadening. The smoothed values, b°(sm), were derived from hand plots for sets of "families" of rotational transitions. Not all lines listed were measured in this study due to blending and/or weakness of the transitions observed in the spectra and these entries were left blank in the table. Also several entries list values for b°(sm) but not b°(obs) (or d°(obs)) which translates that plots of families did not require all of the transitions, however the smoothed values were truncated just a few J's past the last observed values and entries for b°(sm) beyond the cut-off points were left blank in the table. In a few cases, b°(obs) was not obtained for any of the transitions of a family that are represented in the table and no attempt was made to obtain b°(sm) for the set. The N_2-broadened parameters given in table 2 were derived from measurements using the 2.39m long absorption cell whereas the air-broadened results were derived from spectra obtained using longer path lengths and, therefore, there are more entries for the air-broadened coefficients than the N_2-broadened parameters. Lines labeled with an asterisk before the line position represents a doubled absorption. These lines were not

adequately resolved in the low pressure spectra(1) and entries for these lines include one of the two quantum assignments as well as the sum of the strengths of the two comparable transitions. These doubled lines were treated as one absorption in the analysis of the present set of data. This caused only slight errors in the determination of b^{o}(obs) for the majority doubled transitions however the values of d^{o}(obs) for these entries may be in error by a much larger amount than given in the table. The estimated uncertainties in b^{o}(obs) and d^{o}(obs) are given within parentheses after the respective values of these parameters.

Table 3 is an excerpt of a listing, comparable to Table 2 in format, and gives low pressure(1) and air- and N_2-broadened results for the (010)-(000) band of $D_2{}^{16}O$. A few transitions with listed air-broadened values of b^{o}(sm) were derived with measured $D_2{}^{18}O$ lines with the same rotational transitions. For this situation, the $D_2{}^{16}O$ transitions were observed to be too strong to measure in any of the present spectra. Table 4 is a listing of air-broadened values of b^{o}(sm), b^{o}(obs), and d^{o}(obs) for the pure rotational band of $HD^{16}O$ (15 entries), the (010)-(010) band of $HD^{18}O$ and $D_2{}^{18}O$ and the (020)-(010) bands of $HD^{16}O$ and $D_2{}^{16}O$. Values of b^{o}(sm), given in the table, were derived from the analyses of the (010)-(000) bands of $HD^{16}O$ and $D_2{}^{16}O$.

The pressure broadened measurements obtained by Rinsland et al. for HDO(5) and D_2O(6) were not as extensive as given in Tables 2 and 3 because they obtained their results at lower optical densities than used in the present study. The majority of their

measurements(5,6) included transitions with the strongest intensities and a comparison of their values of b^o(obs) for air- and N_2-broadening of HDO and D_2O with the present set of measurements is, on the average, very good. However, the comparison was not that favorable for values of d^o(obs) in which sizable differences were found between their results(5,6) and those given here. This may be due, in part, to differences between the "zero" pressure frequencies used in their analysis and the values used here which were derived from the energy levels given in refs. (1,2).

7. CONCLUSION

Accurate measurements of linewidth and pressure-induced frequency shifts of 609 lines of HDO broadened by air, 655 lines of HDO broadened by N_2, 471 lines of D_2O broadened by air and 422 lines of D_2O broadened by N_2. The study covered the spectral region between 700 and 1940 cm^{-1}. The data were grouped into "families" of rotational transitions from which smoothed values of half-width (HWHM) coefficients, b^o(sm), were derived from hand plots of the observed values, b^o(obs). For a given transition and broadening agent, b^o(obs) was found to be equal or nearly equal to b^o(obs) for the line with the rotational quanta reversed (rotational reversal) for HDO or D_2O transitions in 95% of the observed pairs. The results for the pressure-induced frequency shift coefficients, d^o(obs), were found to have random values within a "family" of rotational transitions and smoothed values of d^o were not derived.

The pressure-broadened values of b^o(sm), b^o(obs), and d^o(obs) were listed along with low pressure results of line positions and strengths for the (010)-(000) bands of $HD^{16}O$(1) and $D_2{}^{16}O$(2). Another listing included values of b^o(obs) and d^o(obs) for 15 lines of the (000)-(000) band of $HD^{16}O$ with other entries for the (010)-(000) bands of $HD^{18}O$ and $H_2{}^{18}O$ and the (020)-(010) bands of $HD^{16}O$ and $D_2{}^{16}O$.

The pressure broadened measurements given by Rinsland et al. for HDO(5) and D_2O(6) were not as extensive as those obtained in this study because the absorption path length they used for both studies(5,6) was lower than any applied in the present study. The majority of their measurements(5,6) included transitions with the strongest intensities and a comparison of their values of b^o(obs) for air- and N_2-broadening of HDO and D_2O with the present set of measurements is, on the average, very good. However, the comparison was not that favorable for values of d^o(obs) in which sizable differences were found between their results(5,6) and those given here. This may be due, in part, to differences between the "zero" pressure frequencies used in the their analysis and the values used here which were derived from the energy levels given in refs. (1,2).

7. ACKNOWLEDGEMENTS

The author wishes to thank the Kitt Peak National Observatory for the use of the FTS and C. Plymate for assistance in obtaining the $HDO/D_2O/H_2O$ spectra. The research described in this paper was

performed at the Jet Propulsion Laboratory, California Institute of Technology, under contract with The National Aeronautics and Space Administration.

REFERENCES

1. R. A. Toth, J. Mol. Spectros. (in press)

2. R. A. Toth, J. Mol. Spectros. (in press)

3. R. A. Toth, J. Mol. Spectrosc. 162, 20-40 (1993).

4. R. A. Toth, J. Mol. Spectrosc. 162, 41-54 (1993).

5. C. P. Rinsland, M. A. Smith, V. M. Devi, and D. C. Benner, J. Mol. Spectros. 150, 640-646 (1991).

6. C. P. Rinsland, M. A. Smith, V. M. Devi, and D. C. Benner, J. Mol. Spectros. 156, 507-511 (1992).

7. R. A. Toth, J. Mol. Spectrosc. 190, 379-396 (1998).

8. L. S. Rothman, R. R. Gamache, R. H. Tipping C. P. Rinsland, M. A. H. Smith, D. C. Benner, V. M. Devi, J.-M. Flaud, C. Camy-Peyret, A. Perrin, A. Goldman, S. T. Massie, L. R. Brown, and R. A. Toth, J. Q. S. R. T. 48, 469-507 (1993).

9. R. A. Toth, J.Q.S.R.T (in press)

10. R. A. Toth, J. Opt. Soc Am. B 9, 462-482 (1992).

11. L. R. Brown and C. Plymate, J. Q. S. R. T. 56, 263-282 (1996).

12. R. A. Toth, L. R. Brown and C. Plymate, JQSRT 59, 529-562 (1998).

FIGURE CAPTIONS

FIG. 1. Unapodized observed and synthetic spectra of D_2O broadened by air at a resolution of 0.005 cm^{-1} covering the lines located at 1182.47 and 1182.80 cm^{-1}. The absorption path length was 73 m and the broadening pressure was 501.6 Torr. The observed spectrum was overlaid with the respective synthetic spectrum, and the residual plot, shown in the upper portion gives the percent differences between the observed and synthetic spectra.

FIG. 2. Unapodized observed and synthetic spectra of D_2O broadened by air at a resolution of 0.005 cm^{-1} covering the comparable transitions located at 957.83 and 958.05 cm^{-1}. The absorption path length was 73 m and the broadening pressure was 501.6 Torr. The observed spectrum was overlaid with the respective synthetic spectrum, and the residual plot, shown in the upper portion gives the percent differences between the observed and synthetic spectra.

FIG. 3. Unapodized observed and synthetic spectra of HDO broadened by air at a resolution of 0.005 cm^{-1} covering the comparable transitions located at 1176.38 and 1176.68 cm^{-1}. The absorption path length was 73 m and the broadening pressure was 501.6 Torr. The observed spectrum was overlaid with the respective synthetic spectrum, and the residual plot, shown in the upper portion gives the percent differences between the observed and synthetic spectra. The two lines show effects due to line mixing particularity in the trough region between the lines. A Voigt line profile was used to compute the synthetic spectrum.

FIG. 4. Unapodized observed and synthetic spectra of HDO broadened

by air at a resolution of 0.005 cm^{-1} covering the comparable transitions located at 1630.66 and 1630.76 cm^{-1}. The absorption path length was 193 m and the broadening pressure was 302.2 Torr. The observed spectrum was overlaid with the respective synthetic spectrum, and the residual plot, shown in the upper portion gives the percent differences between the observed and synthetic spectra. The two lines show effects due to line mixing particularity in the trough region between the lines. A Voigt line profile was used to compute the synthetic spectrum.

FIG. 5 Observed values of air-broadened width coefficients, $b^{\circ}(obs)$, (HWHM) of HDO for four sets of "families" (see text) of rotational transitions. Two sets given in the left panel are related families, one is a P-branch set and the other is a R-branch set. The same for the right panel. Note the similarities between R-branch and P-branch values for upper J (R-branch)= lower J (P-branch)= |m| for the majority of the $b^{\circ}(obs)$ shown in each panel which illustrates the linewidth behavior for rotational reversal (see text). Two examples, one in each panel, illustrate rotational reversal not obeyed in which the values of $b^{\circ}(obs)$ differ by a sizable amount and they are denoted by dashed ovals around the values of $b^{\circ}(obs)$.

FIG. 6 Observed values of air-broadened frequency-shift coefficients, $d^{\circ}(obs)$, of D_2O for four sets of "families" (see text) of rotational transitions. Two sets given in the left panel are related families of Q-branch transitions and the right panel contain two sets of related families of P-branch and R-branch

transitions. Unlike linewidth coefficients, frequency-shift parameters do not obey rotational reversal for the majority of transitions.

Table 1. Experimental conditions of water vapor samples. All samples at or near room temperature (296K).

frequency interval	res. (cm^{-1})	pres. (Torr)	path (m)	percent abundance of isotopic species D_2O	HDO	H_2O	pressure broadening agent	(Torr)
500-2200	0.0054	1.24	25	34.2	48.2	17.6	air	302.2
500-2200	0.0054	1.24	73	34.2	48.2	17.6	air	302.2
500-2200	0.0054	1.24	193	34.2	48.2	17.6	air	302.2
500-2200	0.0054	1.22	193	34.2	48.2	17.6	air	501.6
500-2200	0.0054	1.22	73	34.2	48.2	17.6	air	501.6
500-2200	0.0054	1.22	25	34.2	48.2	17.6	air	501.6
500-2200	0.0054	2.86	2.39	27.2	49.9	22.8	N2	301.3
500-2200	0.0054	1.16	2.39	28.8	49.8	21.5	N2	357.1
500-2200	0.0054	0.94	433	0.0	0.03	99.9	air	249.1
500-2200	0.0054	2.16	193	0.0	0.03	99.9	air	497.8
500-2200	0.0054	2.15	433	0.0	0.03	99.9	air	497.9
500-2200	0.0054	2.99	193	0.0	0.03	99.9	air	396.3
500-2200	0.0054	2.98	433	0.0	0.03	99.9	air	396.3

frequency intervals in cm^{-1} and represent the spectral coverage of the data.

Table 2. Computed line positions, observed strengths, air and N_2-broadening coefficients, b^o, and pressure-induced frequency shifts, d^o, of $HD^{16}O$ in the (010)-(000) band. b^o and d^o in cm^{-1}/atm. $\times 10^4$ at 296K.

computed		upper			lower			observed			air-broadening			N_2-broadening		
position	un	J	K_a	K_c	J	K_a	K_c	strength	%s	(o-c)%	b^o(sm)	b^o(obs.)	d^o(obs.)	b^o(sm)	b^o(obs.)	d^o(obs.)
1420.31275	3.	6	3	4	6	3	3	1.68E-01	1.	1.4	828.	860.(52.)	-13.(4.)	930.	927.(4.)	7.(6.)
1420.65135	3.	2	2	0	3	1	3	5.16E-02	2.	.5	985.	985.(6.)	29.(11.)	1060.	1076.(15.)	8.(14.)
1421.14536	4.	7	2	5	8	1	8	2.66E-03	16.	-.5	860.			910.		
1421.20859	4.	5	2	3	4	3	2	1.35E-01	2.	1.8	863.			970.	965.(20.)	8.(1.)
1421.37812	5.	5	3	3	5	3	2	3.24E-01	2.	1.0	829.			931.	929.(2.)	10.(5.)
1421.60730	2.	3	3	1	3	3	0	1.01E+00	5.	-3.1	823.			925.		
1421.65802	3.	4	3	2	4	3	1	6.00E-01	9.	2.2	830.			768.		
1421.66167	2.	3	3	0	3	3	1	1.05E+00	5.	.8	823.			925.		
1421.83673	5.	7	2	5	8	0	8	9.43E-04	2.	-.2	1000.					
1422.03412	4.	4	3	1	4	3	2	5.82E-01	5.	-1.0	830.			768.	931.(3.)	-17.(4.)
1422.53913	2.	3	1	2	3	1	3	2.15E-01	2.	2.3	956.			1074.	1074.(16.)	27.(4.)
1422.69174	2.	1	1	0	1	0	1	1.22E+00	3.	-3.4	1050.			1180.	1169.(14.)	76.(2.)
1422.85001	4.	5	3	2	5	3	3	3.23E-01	1.	.4	829.			931.	938.(8.)	26.(5.)
1423.03629	5.	6	2	5	5	3	2	1.31E-01	1.	.0	870.			1047.		
1423.05933	3.	5	2	3	5	2	4	1.89E-01	1.	1.8	916.			1029.		
1423.17918	9.	9	4	5	10	2	8	2.25E-04	4.	-7.9						
1423.83205	6.	9	5	5	10	4	6	6.30E-04	30.	14.5	700.			603.		
1423.88486	3.	4	3	1	5	2	4	3.22E-02	5.	-2.0	890.	873.(45.)	2.(5.)	1000.		
1424.56842	3.	6	3	3	6	3	4	1.69E-01	1.	1.3	828.	815.(33.)	18.(6.)	930.	921.(11.)	36.(1.)
1425.80619	5.	7	3	5	6	4	2	5.33E-02	2.	-2.8	820.	829.(55.)	-9.(8.)	875.	878.(11.)	9.(6.)
1426.02452	2.	2	1	1	2	0	2	1.57E+00	3.	-3.5	1032.	999.(30.)	45.(6.)	1160.	1132.(34.)	47.(4.)
1426.59437	6.	8	4	5	7	5	2	1.67E-02	4.	.3	790.	790.(20.)	-8.(11.)	731.	707.(71.)	50.(50.)
*1427.05202	11.	10	7	4	9	8	1	2.69E-04	4.	-1.6						
1427.18446	4.	6	4	3	7	3	4	7.80E-03	5.	-7.9	821.	863.(86.)	-15.(20.)	940.	915.(92.)	-111.(111.)
1427.37418	6.	8	4	4	7	5	3	1.75E-02	4.	5.1	720.	710.(71.)	-11.(12.)	768.	783.(78.)	-72.(72.)
1427.84985	4.	7	3	4	7	3	5	8.12E-02	1.	.6	840.	839.(17.)	20.(3.)	925.	930.(4.)	23.(1.)
1428.66211	8.	12	2	11	11	3	8	1.85E-03	6.	1.9	810.	760.(61.)	-47.(3.)	820.		
1428.93150	8.	11	4	8	11	4	7	2.79E-03	5.	-.2	720.			668.		
1429.58792	7.	9	5	5	8	6	2	3.93E-03	2.	-1.5	720.					
1429.71201	3.	2	2	0	3	0	3	2.57E-03	10.	-.4	1000.					
1430.86382	5.	7	3	4	6	4	3	5.41E-02	2.	-1.8	821.	816.(16.)	-13.(2.)	940.	936.(22.)	-6.(4.)
1431.59979	2.	3	1	2	3	0	3	1.50E+00	5.	-2.3	1001.	948.(95.)	44.(20.)	1125.	1112.(6.)	48.(2.)
1432.02548	4.	6	2	4	6	2	5	9.00E-02	3.	-3.0	910.	953.(95.)	-32.(50.)	990.	960.(96.)	41.(41.)
1432.31615	4.	6	4	2	7	3	5	8.31E-03	16.	3.1	820.	725.(58.)	13.(7.)	875.		
1432.59633	5.	10	4	7	10	4	6	7.71E-03	0.	.9	680.	675.(27.)	-15.(7.)	721.		
1432.82241	2.	3	3	1	4	2	2	2.34E-02	4.	1.0	899.	891.(9.)	12.(5.)	992.	944.(94.)	35.(35.)
1433.43456	6.	8	3	5	8	3	6	3.69E-02	3.	2.1	780.	810.(65.)	33.(20.)	876.	865.(25.)	65.(16.)
1433.59840	4.	7	2	6	6	3	3	1.03E-01	2.	-1.3	940.	970.(58.)	2.(8.)	970.		
1433.63068	6.	8	2	6	9	1	9	7.25E-04	15.	-3.3	820.			872.		
1433.66276	3.	4	1	3	4	1	4	1.22E-01	2.	-.4	973.			1093.		
1433.69657	1.	2	1	2	1	1	1	7.34E-01	4.	2.4	971.	1014.(101.)	-12.(20.)	1091.	1098.(3.)	6.(11.)
1434.00876	4.	5	3	2	6	1	5	1.83E-03	4.	-2.4						
1434.28592	3.	2	0	2	1	0	1	1.02E+00	3.	.7	971.	871.(87.)	0.(0.)	1091.	1090.(4.)	39.(3.)
1434.47414	5.	9	4	6	9	4	5	1.95E-02	3.	2.1	732.			788.		
1434.65599	3.	4	1	3	3	2	2	3.72E-01	2.	1.1	959.			1077.		
1434.68534	9.	4	4	1	4	4	0	5.96E-01	4.	-6.9	616.			692.	698.(8.)	31.(7.)
1434.68888	5.	4	4	0	4	4	1	6.08E-01	4.	-4.9	616.			692.	698.(8.)	62.(38.)
1434.92880	5.	5	4	2	5	4	1	3.55E-01	4.	.3	649.			729.	729.(73.)	34.(7.)
1434.96012	4.	5	4	1	5	4	2	3.55E-01	3.	.3	649.			729.	729.(73.)	20.(12.)
1435.17593	4.	6	4	3	6	4	2	1.86E-01	1.	-.8	684.			768.	788.(79.)	5.(5.)
1435.21477	5.	8	4	5	8	4	4	4.37E-02	6.	-.5	731.			821.		
1435.30007	3.	1	1	1	0	0	0	9.48E-01	5.	.1	1013.			1138.		
1435.33012	6.	6	4	2	6	4	3	1.87E-01	2.	-.3	684.			768.		
1435.33512	6.	7	4	4	7	4	3	9.41E-02	5.	.3	724.			813.		
1435.43606	21.	10	6	5	9	7	2	7.55E-04	8.	-1.3	600.					
1435.44492	10.	10	6	4	9	7	3	7.29E-04	6.	-4.8	650.					
1435.88745	5.	7	4	3	7	4	4	9.32E-02	1.	-.8	724.	740.(38.)	-25.(12.)	813.	814.(12.)	0.(0.)
*1437.25803	28.	11	8	3	10	9	2	3.71E-05	2.	.6	500.					
1437.64349	2.	3	3	0	4	2	3	2.20E-02	4.	.6	880.	884.(38.)	21.(12.)	972.	938.(94.)	24.(24.)

b^o(sm) is a smoothed value for b^o derived from hand drawn plots of b^o(obs.) relegated in terms of "families" of transitions
Line positions and un in cm^{-1}. un is the estimated uncertainty in the computed position.
The computed values are derived from the energy levels given in Table 2 of ref. 1. and un is multiplied by 10^5
Line strengths in cm^{-2}/atm. at 296K and are from ref. 1
%s are the estimated uncertainties in the measured line strengths in percent.
(o-c)%, observed minus computed line strength values given in percent. Computed values are derived from constants given in ref 1
*asterisks denote doubled absorptions with the quantum assignment given for one of the transitions
The strength given represents the sum of the strengths of the two comparable transitions.
Strengths normalized to 99.9% $HD^{16}O$.
Values given within parentheses are estimated uncertainties in the last digits

Table 3. Computed line positions, observed strengths, air and N_2-broadening coefficients, b^o, and pressure-induced frequency shifts, d^o, of $D_2{}^{16}O$ in the (010)-(000) band. b^o and d^o in $cm^{-1}/atm. \times 10^4$ at 296K.

computed		upper			lower			observed			air-broadening			N_2-broadening		
position	un	J	K_a	K_c	J	K_a	K_c	strength	%s	(o-c)%	b^o(sm)	b^o(obs.)	d^o(obs.)	b^o(sm)	b^o(obs.)	d^o(obs.)
998.75758	10.	8	5	4	9	6	3	5.28E-02	3.	-2.9	730.	729.(7.)	-3.(1.)	850.	880.(88.)	32.(32.)
998.88930	12.	8	5	3	9	6	4	9.96E-02	7.	-8.7	739.	725.(9.)	4.(1.)	830.	814.(5.)	-7.(8.)
999.60854	4.	3	1	2	4	4	1	4.64E-04	5.	8.4	992.					
999.61708	22.	16	3	13	17	4	14	4.33E-04	6.	-2.0						
1001.81422	8.	5	2	3	5	5	0	1.00E-04	10.	11.8	840.					
*1002.11360	19.	16	0	16	17	1	17	8.70E-03	5.	.0	305.	307.(4.)	-11.(3.)	320.	334.(33.)	-2.(2.)
*1003.52302	13.	7	7	1	8	8	0	1.38E-01	6.	-.2	432.	435.(22.)	-15.(10.)	485.	482.(7.)	-18.(9.)
1005.03263	17.	16	1	15	17	2	16	2.24E-03	1.	-3.9	370.	560.(50.)	1.(10.)	302.		
1005.05812	12.	16	2	15	17	1	16	1.15E-03	5.	-1.3	332.			290.		
1005.07756	13.	8	4	5	9	5	4	6.22E-02	2.	-1.3	790.	785.(63.)	-4.(2.)	929.	981.(98.)	-24.(24.)
1005.11703	12.	16	2	14	17	3	15	1.10E-03	15.	10.2	390.					
1005.28507	23.	15	3	12	16	4	13	5.39E-04	6.	3.5	650.					
1005.66795	67.	16	3	14	17	2	15	5.20E-04	3.	4.8	380.					
1006.06343	10.	8	3	6	9	4	5	4.95E-02	1.	-5.9	857.	882.(18.)	-21.(7.)	963.		
1006.09673	21.	16	4	13	17	3	14	2.14E-04	5.	-.3	500.					
1006.15182	8.	5	0	5	6	3	4	1.35E-02	10.	-6.3	940.	920.(55.)	41.(25.)	1000.		
*1006.19153	14.	7	6	2	8	7	1	1.99E-01	4.	-4.4	560.			699.		
1006.38727	6.	6	1	6	6	4	3	5.81E-04	3.	4.1						
1007.35094	9.	6	2	4	6	5	1	6.46E-04	4.	-1.2	830.					
1007.57765	6.	8	4	4	9	5	5	1.23E-01	1.	-2.9	826.	825.(5.)	2.(1.)	928.	883.(4.)	22.(7.)
*1008.55281	21.	17	1	17	17	2	16	2.10E-03	5.	3.8	365.	365.(7.)	37.(4.)			
1008.58899	50.	20	1	19	20	2	18	7.92E-05	6.	6.6	220.					
1009.78319	13.	14	3	11	15	4	12	2.44E-03	2.	5.1	700.	703.(27.)	-51.(10.)	603.		
1010.40825	8.	6	1	6	7	2	5	2.55E-02	5.	5.6	936.	931.(45.)	10.(20.)	1052.		
1010.49205	13.	12	2	10	12	5	7	1.32E-03	4.	.4	740.					
1010.91615	7.	7	5	3	8	6	2	1.79E-01	3.	-4.5	743.			835.	838.(16.)	72.(19.)
1010.94749	9.	7	5	2	8	6	3	9.02E-02	1.	-3.7	676.			760.	745.(26.)	68.(30.)
1011.97222	6.	7	2	6	8	3	5	9.36E-02	2.	-3.6	925.	933.(14.)	-2.(3.)	1022.	1040.(104.)	-8.(8.)
*1012.82050	18.	15	1	15	16	0	16	1.85E-02	4.	-.2	347.	352.(9.)	-6.(4.)	390.	389.(39.)	-8.(8.)
1013.04106	10.	13	3	10	14	4	11	2.49E-03	6.	1.7	750.	682.(5.)	-5.(3.)	690.		
1013.31731	11.	7	2	5	7	5	2	7.19E-04	7.	-1.1	820.					
1013.71484	22.	15	2	13	16	3	14	1.12E-03	6.	-1.9	460.	444.(22.)	-37.(3.)			
1014.73999	11.	15	3	13	16	2	14	2.30E-03	8.	1.1	435.					
1014.75350	12.	15	1	14	16	2	15	2.58E-03	5.	-.3	405.	404.(20.)	50.(50.)	360.		
1014.80434	12.	15	2	14	16	1	15	5.23E-03	4.	1.0	378.	360.(18.)	-25.(13.)	360.		
1015.31291	10.	12	3	9	13	4	10	1.04E-02	4.	5.0	808.	807.(12.)	-17.(8.)	780.		
1016.09122	18.	15	4	12	16	3	13	1.03E-03	10.	4.2	550.					
1017.16563	9.	11	3	8	12	4	9	9.77E-03	4.	1.0	825.	822.(25.)	-19.(4.)	858.		
1017.69383	11.	7	4	4	8	5	3	2.14E-01	0.	-3.3	796.	815.(33.)	3.(3.)	894.	895.(5.)	5.(6.)
1018.03701	4.	5	1	5	5	4	2	8.46E-04	11.	3.1						
*1018.48284	21.	6	6	0	7	7	1	3.14E-01	2.	-7.4	536.			602.	595.(3.)	4.(6.)
1018.51232	202.	19	2	18	19	3	17	2.00E-04	15.	1.7	240.					
1018.54194	50.	19	1	18	19	2	17	1.00E-04	15.	1.7	280.					
1018.56781	9.	7	4	3	8	5	4	1.05E-01	1.	-5.3	810.	830.(83.)	-1.(10.)	910.	909.(28.)	6.(13.)
1018.71395	9.	8	2	6	8	5	3	2.49E-03	4.	2.4	800.	800.(80.)	2.(10.)			
1019.22728	6.	11	2	9	11	5	6	1.20E-03	10.	1.4	760.					
1019.30765	8.	10	3	7	11	4	8	3.75E-02	6.	1.5	860.	874.(15.)	-3.(4.)	881.	978.(98.)	-48.(48.)
1019.44904	16.	10	1	9	10	4	6	4.01E-03	5.	3.9	850.	840.(59.)	20.(7.)			
1019.63486	18.	16	1	16	16	2	15	1.46E-03	5.	-2.0	375.	370.(44.)	40.(30.)			
1019.64505	16.	16	0	16	16	1	15	2.90E-03	5.	-2.7	370.	370.(11.)	10.(30.)	450.		
1022.03567	12.	14	2	12	15	3	13	5.00E-03	10.	.6	520.	500.(50.)	-29.(15.)	570.		
1022.34048	9.	9	2	7	9	5	4	1.65E-03	4.	4.3	790.					
1022.41915	15.	9	3	6	10	4	7	3.55E-02	6.	2.9	860.	885.(22.)	2.(30.)	899.	858.(86.)	45.(45.)
1022.90031	6.	10	2	8	10	5	5	3.14E-03	3.	-.4	780.	785.(78.)	-32.(20.)			
1022.99426	5.	7	3	5	8	4	4	2.01E-01	1.	-1.9	877.	880.(41.)	-30.(7.)	985.	988.(6.)	-16.(6.)
1023.14440	21.	6	5	2	7	6	1	1.50E-01	1.	-1.3	703.			790.	800.(80.)	30.(30.)
1023.14979	13.	6	5	1	7	6	2	2.88E-01	3.	-5.3	710.			798.	789.(11.)	3.(22.)
1023.45553	13.	14	0	14	15	1	15	2.50E-02	5.	-.3	411.	402.(16.)	10.(20.)	462.	440.(44.)	-15.(15.)

b^o(sm) is a smoothed value for b^o derived from hand drawn plots of b^o(obs.) relegated in terms of "families" of transitions
Line positions and un in cm^{-1}. un is the estimated uncertainty in the computed position.
The computed values are derived from the energy levels given in Table 1 of ref. 2. and un is multiplied by 10^5
Line strengths in $cm^{-2}/atm.$ at 296K and are from ref. 2
%s are the estimated uncertainties in the measured line strengths in percent.
(o-c)%, observed minus computed line strength values given in percent. Computed values are derived from constants given in ref 1
*asterisks denote doubled absorptions with the quantum assignment given for the stonger of the two transitions
The strength given represents the sum of the strengths of the two comparable transitions.
Strengths normalized to 99.9% $D_2{}^{16}O$
Values given within parentheses are estimated uncertainties in the last digits.

Table 4. Computed line positions and air-broadening coefficients, b^o, and pressure-induced frequency shifts, d^o, of D_2O and HDO. b^o and d^o in $cm^{-1}/atm. \times 10^4$ at 296K.

computed	upper			lower			air-broadening					
position	J	K_a	K_c	J	K_a	K_c	b^o(sm)	b^o(obs.)	d^o(obs.)	mol	iso	band
709.81142	12	6	7	11	1	10	680.	736.(74.)	31.(20.)	HDO	16	1 1
725.49276	13	5	9	12	0	12	740.	740.(74.)	67.(50.)	HDO	16	1 1
731.94109	11	8	4	10	5	5	640.	645.(32.)	-15.(8.)	HDO	16	1 1
732.23588	11	8	3	10	5	6	680.	683.(14.)	-59.(12.)	HDO	16	1 1
736.30082	15	4	11	14	1	14	855.	846.(85.)	97.(80.)	HDO	16	1 1
738.09597	13	6	8	12	1	11	628.	624.(19.)	45.(14.)	HDO	16	1 1
743.69689	12	8	5	11	5	6	689.	690.(31.)	-45.(15.)	HDO	16	1 1
744.45010	12	8	4	11	5	7	680.	683.(20.)	-11.(5.)	HDO	16	1 1
754.47564	13	8	6	12	5	7	738.	735.(15.)	-25.(12.)	HDO	16	1 1
756.20777	13	8	5	12	5	8	680.	719.(36.)	4.(60.)	HDO	16	1 1
767.57617	14	8	6	13	5	9	680.	677.(68.)	81.(30.)	HDO	16	1 1
769.74581	14	6	9	13	1	12	608.	650.(45.)	70.(60.)	HDO	16	1 1
771.67679	15	8	8	14	5	9	827.	811.(81.)	6.(10.)	HDO	16	1 1
771.85866	14	5	10	13	0	13	680.	637.(64.)	-10.(20.)	HDO	16	1 1
825.96929	14	7	8	13	2	11	700.	714.(71.)	-16.(20.)	HDO	16	1 1
989.04356	8	6	2	9	7	3	668.	631.(63.)	-20.(30.)	D2O	18	2 1
997.70087	6	5	1	7	6	2	710.	635.(19.)	-18.(11.)	D2O	16	3 2
1000.46925	8	3	5	9	4	6	881.	900.(36.)	-6.(80.)	D2O	16	3 2
1001.25765	7	6	2	8	7	1	560.	560.(17.)	18.(9.)	D2O	18	2 1
1004.29043	6	4	3	7	5	2	755.	725.(43.)	6.(10.)	D2O	16	3 2
1004.48871	6	4	2	7	5	3	776.	760.(23.)	14.(8.)	D2O	16	3 2
1010.06792	5	5	1	6	6	0	632.	548.(16.)	-14.(7.)	D2O	16	3 2
1013.53966	6	6	0	7	7	1	536.	488.(10.)	-18.(4.)	D2O	18	2 1
1024.66735	6	4	2	7	5	3	776.	810.(65.)	32.(25.)	D2O	18	2 1
1025.64251	5	3	3	6	4	2	877.	880.(40.)	36.(5.)	D2O	16	3 2
1031.06823	5	2	4	6	3	3	920.	920.(28.)	-48.(7.)	D2O	16	3 2
1036.65906	5	4	2	6	5	1	754.	710.(71.)	13.(13.)	D2O	18	2 1
1036.71755	5	4	1	6	5	2	752.	732.(22.)	31.(25.)	D2O	18	2 1
1038.34239	4	3	2	5	4	1	865.	850.(42.)	-39.(12.)	D2O	16	3 2
1038.69876	4	3	1	5	4	2	900.	834.(8.)	-5.(5.)	D2O	16	3 2
1044.93188	5	3	3	6	4	2	877.	852.(68.)	-20.(5.)	D2O	18	2 1
1046.72436	5	3	2	6	4	3	872.	837.(84.)	10.(8.)	D2O	18	2 1
1047.80548	4	2	3	5	3	2	920.	895.(45.)	-42.(3.)	D2O	16	3 2
1048.94913	4	4	0	5	5	1	733.	760.(61.)	-35.(2.)	D2O	18	2 1
1058.12821	4	3	1	5	4	2	900.	827.(33.)	6.(4.)	D2O	18	2 1
1058.97135	10	0	10	10	1	9	660.	660.(26.)	-18.(10.)	D2O	16	3 2
1059.72482	6	2	4	7	3	5	910.	836.(84.)	12.(4.)	D2O	18	2 1
1062.34297	3	2	2	4	3	1	910.	913.(9.)	-24.(4.)	D2O	16	3 2
1066.83784	8	1	8	9	0	9	788.	780.(23.)	-42.(9.)	D2O	16	3 2
1067.95903	9	0	9	10	1	10	729.	658.(26.)	17.(20.)	D2O	18	2 1
1069.75558	6	1	5	7	2	6	917.	940.(47.)	-44.(7.)	D2O	16	3 2
1071.07352	8	1	7	9	2	8	850.	850.(59.)	-29.(8.)	D2O	18	2 1
1076.91339	7	1	7	8	0	8	832.	790.(39.)	-12.(20.)	D2O	16	3 2
1081.11159	4	1	3	5	2	4	961.	980.(69.)	-21.(7.)	D2O	16	3 2
1082.06722	3	1	3	4	2	2	932.	950.(85.)	-59.(15.)	D2O	18	2 1
1087.85115	7	0	7	8	1	8	815.	800.(80.)	22.(10.)	D2O	18	2 1
1088.27341	7	1	7	8	0	8	832.	778.(62.)	28.(30.)	D2O	18	2 1
1093.54983	2	2	1	3	3	0	900.	898.(13.)	13.(20.)	D2O	18	2 1
1094.09707	2	2	0	3	3	1	943.	942.(38.)	-19.(8.)	D2O	18	2 1
1115.63824	4	0	4	5	1	5	926.	840.(34.)	5.(4.)	D2O	18	2 1
1129.65865	6	1	5	6	2	4	926.	950.(28.)	-35.(20.)	D2O	16	3 2
1130.57814	3	1	3	4	0	4	938.	836.(84.)	10.(6.)	D2O	18	2 1
1134.65513	4	1	3	4	2	2	961.	950.(38.)	-32.(8.)	D2O	16	3 2
1172.99759	2	0	2	1	1	1	1015.	1025.(72.)	-49.(8.)	D2O	16	3 2
1173.77201	6	5	2	7	6	1	514.	482.(10.)	29.(7.)	HDO	18	2 1
1174.96961	2	1	1	2	0	2	1041.	1035.(10.)	39.(7.)	D2O	16	3 2
1185.98494	3	0	3	2	1	2	935.	980.(49.)	11.(7.)	D2O	16	3 2
1186.70221	4	4	0	5	5	1	541.	520.(10.)	-22.(5.)	HDO	16	3 2
1196.55233	6	2	4	6	1	5	926.	910.(45.)	65.(4.)	D2O	16	3 2
1200.68375	2	1	2	1	0	1	1006.	920.(92.)	54.(20.)	D2O	18	2 1
1200.90717	5	4	2	6	5	1	639.	555.(11.)	30.(70.)	HDO	18	2 1
1200.92436	5	4	1	6	5	2	643.	555.(11.)	20.(50.)	HDO	18	2 1
1201.14520	6	3	4	7	4	3	785.	700.(42.)	11.(10.)	HDO	18	2 1

Table 4. continued

computed position	upper J	K_a	K_c	lower J	K_a	K_c	b^o(sm)	b^o(obs.)	d^o(obs.)	mol	iso	band
1203.62452	6	3	3	7	4	4	815.	774.(12.)	-22.(40.)	HDO	18	2 1
1204.93875	6	2	4	6	1	5	926.	940.(47.)	41.(5.)	D2O	18	2 1
1212.50372	6	3	3	6	2	4	900.	893.(36.)	-29.(6.)	D2O	16	3 2
1215.83138	4	4	0	5	5	1	541.	572.(3.)	-28.(4.)	HDO	18	2 1
1217.14988	4	1	4	3	0	3	944.	903.(27.)	44.(20.)	D2O	18	2 1
1220.42588	6	0	6	5	1	5	888.	863.(26.)	-27.(20.)	D2O	16	3 2
1241.78529	7	0	7	6	1	6	866.	850.(38.)	-2.(20.)	D2O	18	2 1
1246.83293	3	3	1	4	4	0	773.	685.(55.)	50.(200.)	HDO	18	2 1
1246.86262	3	3	0	4	4	1	770.	685.(55.)	-10.(30.)	HDO	18	2 1
1274.26843	8	0	8	9	1	9	676.	660.(33.)	-42.(4.)	HDO	18	2 1
1275.44579	8	1	8	9	0	9	664.	610.(18.)	13.(9.)	HDO	18	2 1
1290.01687	6	2	4	7	2	5	873.	735.(29.)	20.(50.)	HDO	18	2 1
1290.38455	4	1	3	5	2	4	950.	800.(64.)	-10.(100.)	HDO	18	2 1
1290.69871	6	1	5	7	1	6	856.	852.(13.)	-51.(7.)	HDO	18	2 1
1302.40689	4	0	4	5	1	5	926.	810.(24.)	27.(12.)	HDO	16	3 2
1303.86197	5	1	4	6	1	5	892.	810.(16.)	10.(40.)	HDO	18	2 1
1322.96209	1	1	0	2	2	1	1003.	970.(58.)	55.(40.)	HDO	18	2 1
1323.11391	4	2	2	5	2	3	908.	873.(70.)	-40.(30.)	HDO	18	2 1
1350.90251	3	0	3	3	1	2	1001.	1045.(31.)	-80.(25.)	HDO	16	3 2
1366.80662	0	0	0	1	1	1	1013.	1025.(31.)	-82.(15.)	HDO	18	2 1
1376.64755	2	0	2	2	1	1	1032.	950.(85.)	-20.(100.)	HDO	18	2 1
1403.75766	2	1	1	2	0	2	1032.	1000.(70.)	29.(20.)	HDO	16	3 2
1406.28415	3	2	1	3	2	2	926.	950.(95.)	32.(25.)	HDO	18	2 1
1415.17392	1	1	0	1	0	1	1050.	985.(15.)	65.(15.)	HDO	18	2 1
1415.30973	5	3	2	5	3	3	829.	783.(16.)	-25.(15.)	HDO	18	2 1
1442.25665	5	5	0	5	5	1	501.	510.(25.)	-37.(25.)	HDO	18	2 1
1442.55539	6	5	2	6	5	1	567.	550.(60.)	-20.(50.)	HDO	18	2 1
1444.44117	3	2	1	3	1	2	964.	931.(19.)	-15.(7.)	HDO	18	2 1
1446.20099	4	0	4	3	1	3	943.	896.(6.)	10.(50.)	HDO	18	2 1
1461.85646	5	0	5	4	1	4	910.	864.(22.)	-10.(30.)	HDO	18	2 1
1466.40952	5	1	5	4	1	4	900.	900.(63.)	10.(7.)	HDO	18	2 1
1478.45239	7	7	1	7	7	0	319.	240.(7.)	-81.(40.)	HDO	18	2 1
1482.30798	5	1	4	4	1	3	921.	800.(64.)	-11.(8.)	HDO	18	2 1
1493.82500	7	1	7	6	0	6	829.	791.(16.)	11.(20.)	HDO	18	2 1
1502.99998	8	0	8	7	1	7	743.	728.(7.)	6.(3.)	HDO	18	2 1
1514.37712	5	2	4	4	1	3	950.	830.(41.)	10.(80.)	HDO	18	2 1
1527.91077	10	1	10	9	0	9	600.	610.(12.)	11.(8.)	HDO	18	2 1
1550.60841	12	1	12	11	0	11	431.	300.(45.)	10.(10.)	HDO	18	2 1
1551.87374	5	2	3	4	1	4	955.	865.(17.)	22.(16.)	HDO	18	2 1
1586.63342	7	3	5	6	2	4	862.	882.(88.)	-28.(20.)	HDO	18	2 1
1589.20001	6	3	3	5	2	4	873.	800.(32.)	44.(10.)	HDO	18	2 1
1594.07176	4	4	1	3	3	0	770.	640.(51.)	20.(100.)	HDO	18	2 1
1594.10196	4	4	0	3	3	1	773.	640.(51.)	20.(100.)	HDO	18	2 1
1625.48487	6	4	2	5	3	3	808.	800.(96.)	-8.(50.)	HDO	18	2 1
1713.38247	6	6	0	5	5	1	450.	435.(22.)	-75.(8.)	HDO	18	2 1

b^o(sm) is a smoothed value for b^o derived from hand drawn plots of b^o(obs.) relegated in terms of "families" of transitions

Line positions in cm^{-1} .Computed valued derived from energy levels given in refs. 1-4

Band notation is as follows: 1=(000) state, 2=(010) state, and 3=(020) state. upper state given first above.

Values given within parentheses are estimated uncertainties in the last digits.

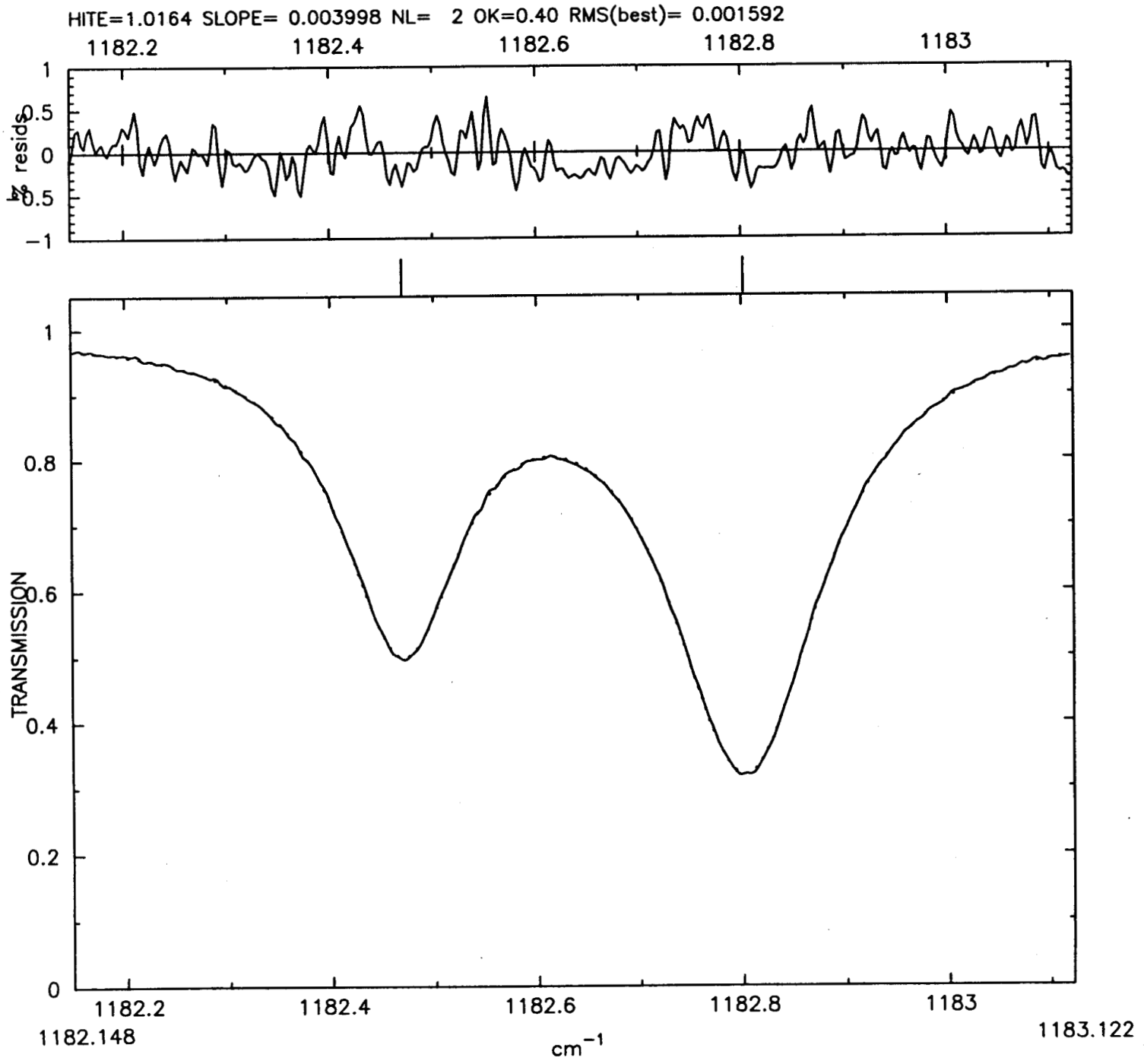
HITE=1.0164 SLOPE= 0.003998 NL= 2 OK=0.40 RMS(best)= 0.001592
1182.2
1182.4
1182.6
1182.8
1183
1
0.5
0
−0.5
−1
% resids
1
0.8
0.6
0.4
0.2
0
TRANSMISSION
1182.2
1182.4
1182.6
1182.8
1183
1182.148
1183.122
cm−1

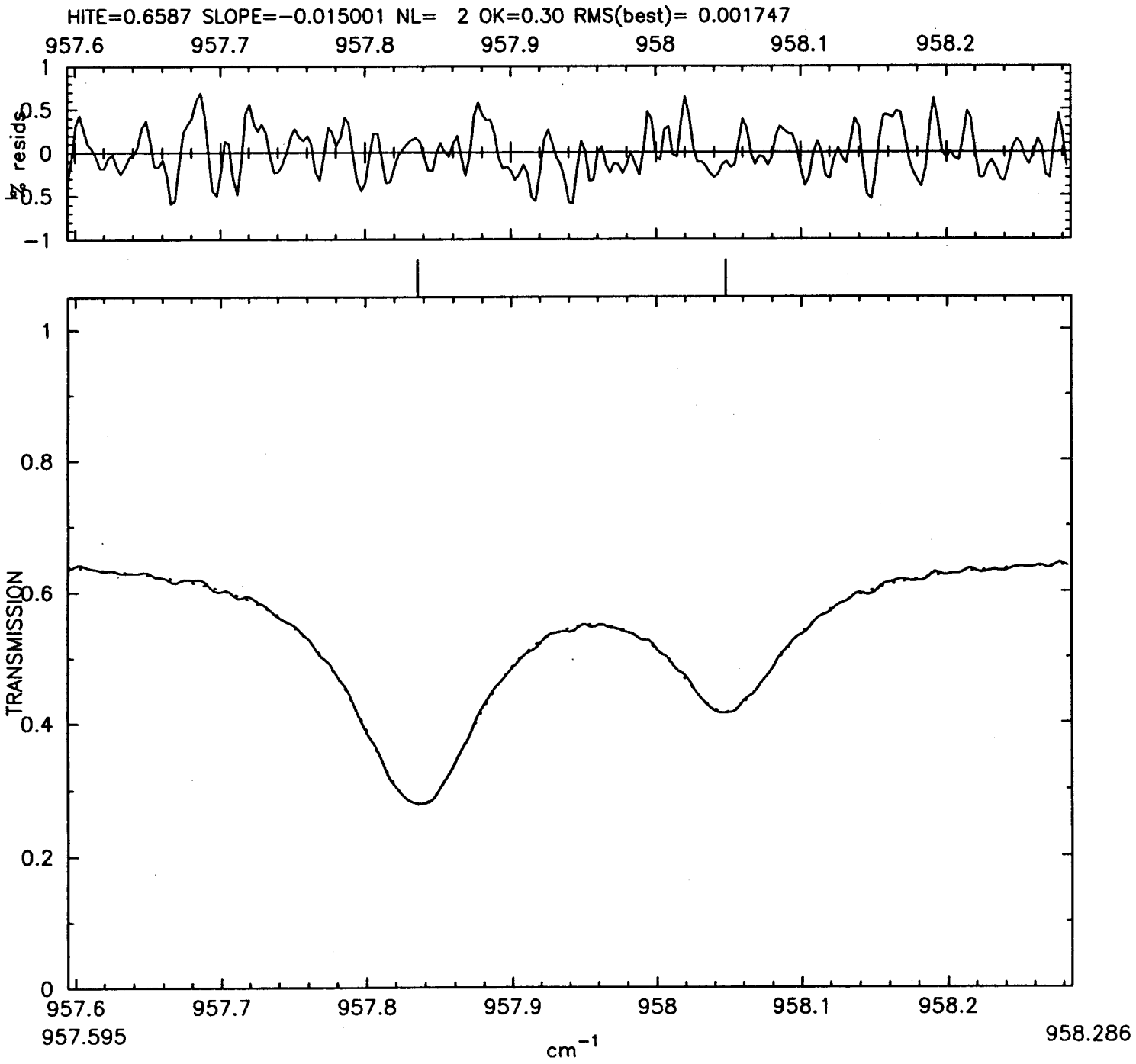
HITE=0.6587 SLOPE=-0.015001 NL= 2 OK=0.30 RMS(best)= 0.001747
957.6
957.7
957.8
957.9
958
958.1
958.2
1
0.5
0
-0.5
-1
% resids
1
0.8
0.6
0.4
0.2
0
TRANSMISSION
957.595
958.286
cm-1

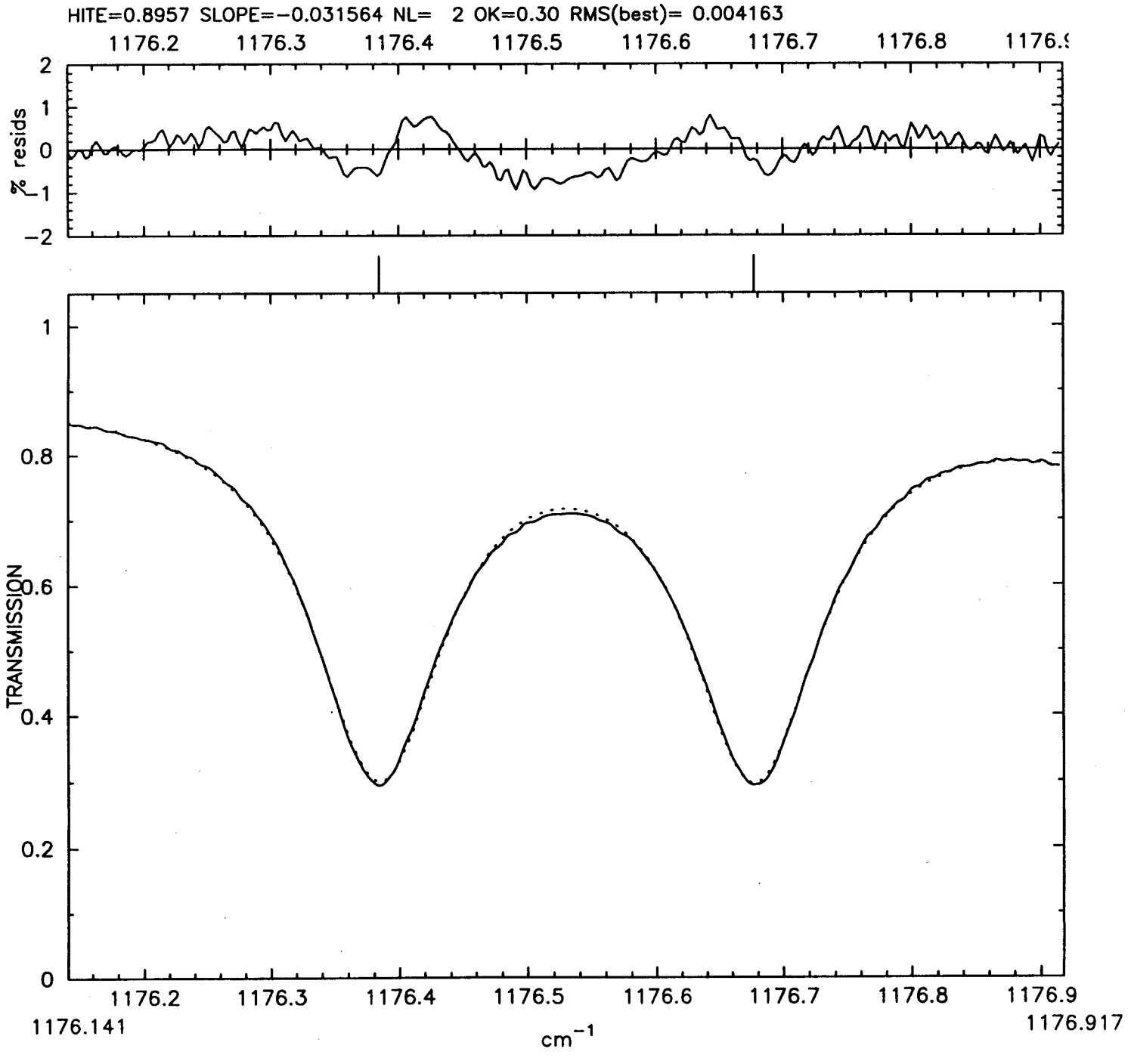
HITE=0.8957 SLOPE=-0.031564 NL= 2 OK=0.30 RMS(best)= 0.004163
1176.2
1176.3
1176.4
1176.5
1176.6
1176.7
1176.8
% resids
2
1
0
−1
−2
TRANSMISSION
1
0.8
0.6
0.4
0.2
0
1176.141
1176.917
cm−1

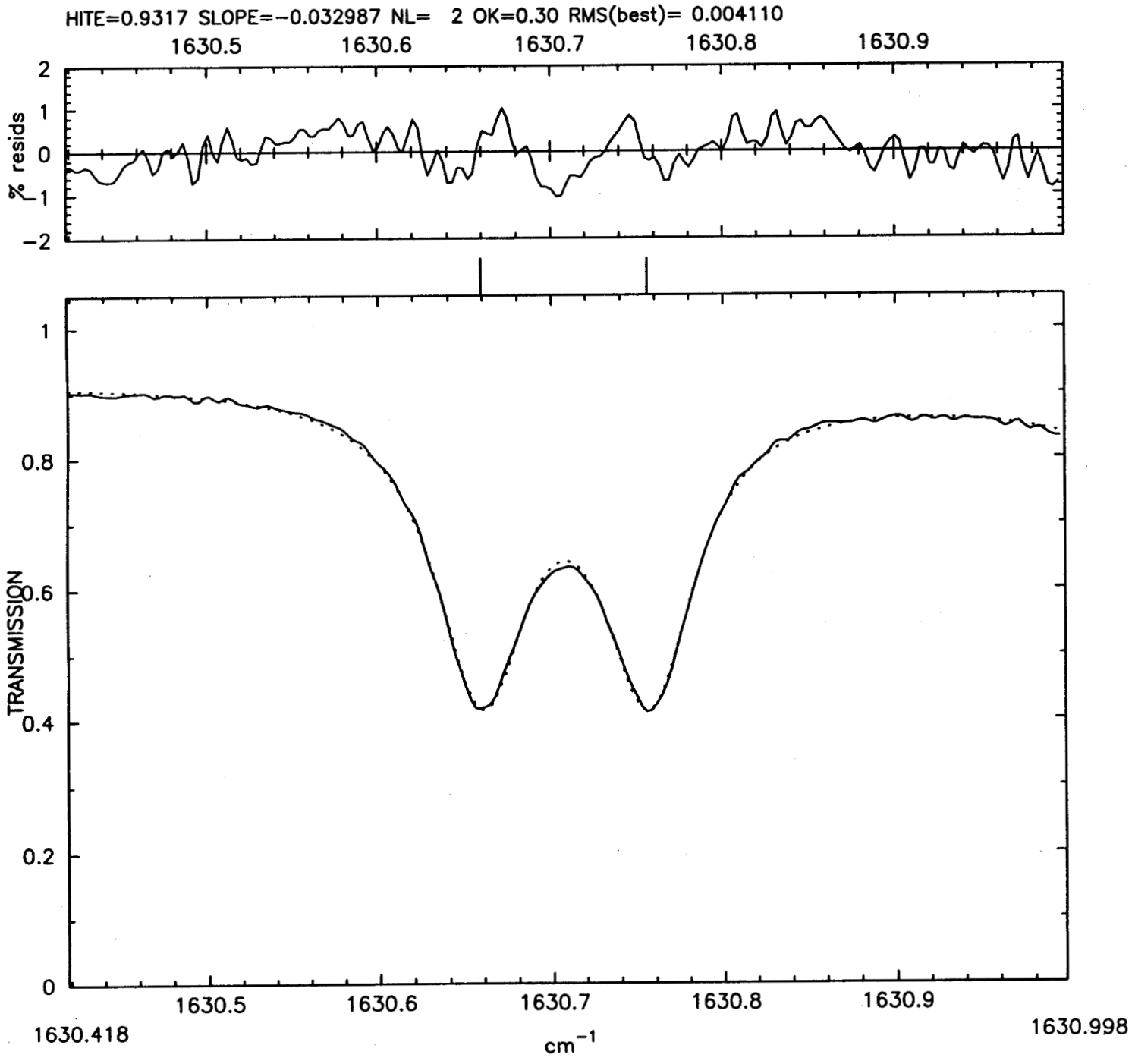
HITE=0.9317 SLOPE=-0.032987 NL= 2 OK=0.30 RMS(best)= 0.004110
1630.5
1630.6
1630.7
1630.8
1630.9
% resids
2
1
0
−1
−2
TRANSMISSION
1
0.8
0.6
0.4
0.2
0
1630.418
1630.998
cm−1

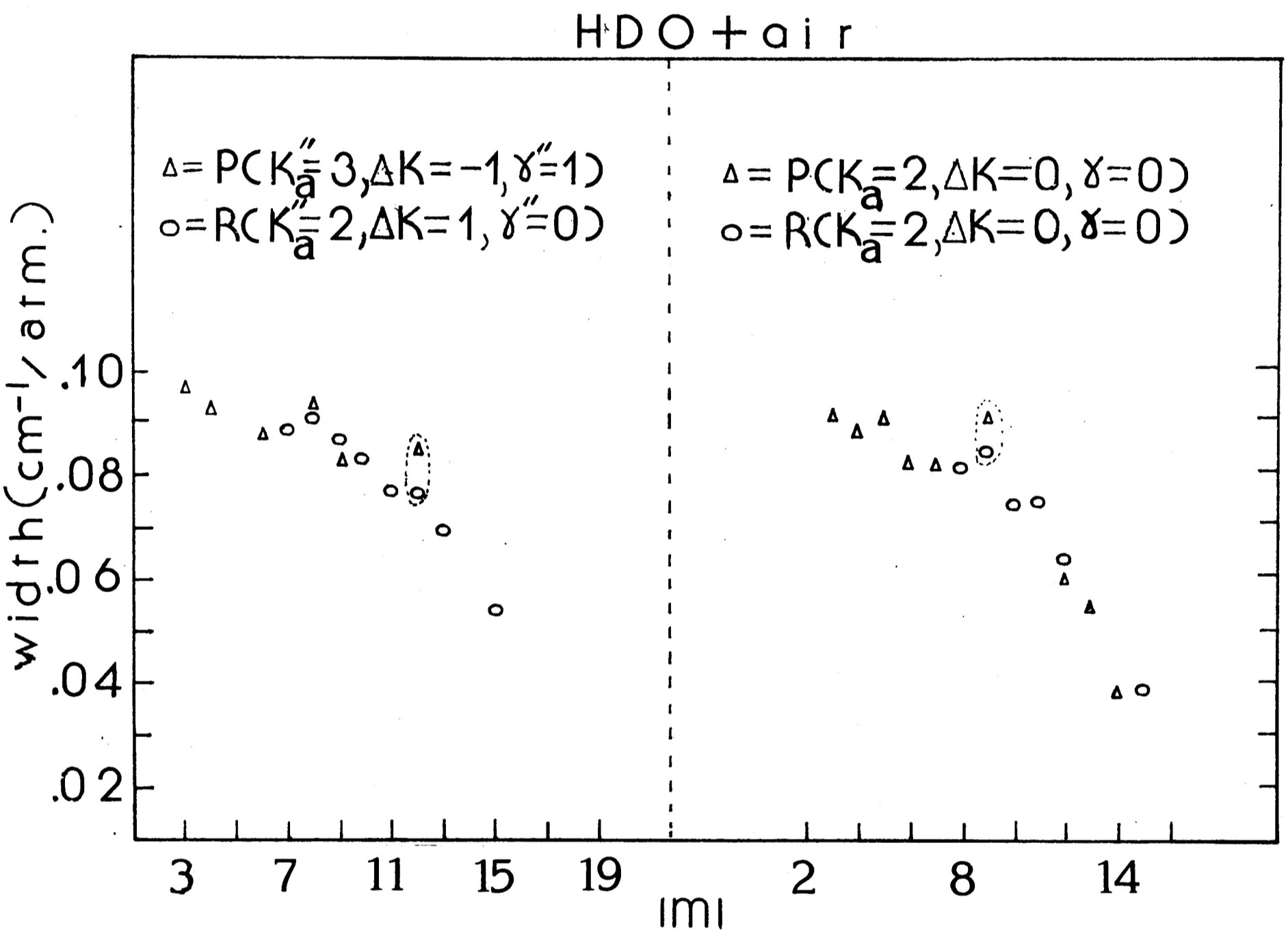
HDO + air
Δ = P(K″a = 3, ΔK = −1, γ″ = 1)
○ = R(K″a = 2, ΔK = 1, γ″ = 0)
Δ = P(Ka = 2, ΔK = 0, γ = 0)
○ = R(Ka = 2, ΔK = 0, γ = 0)
width (cm⁻¹/atm.)
.10
.08
.06
.04
.02
3
7
11
15
19
2
8
14
|m|

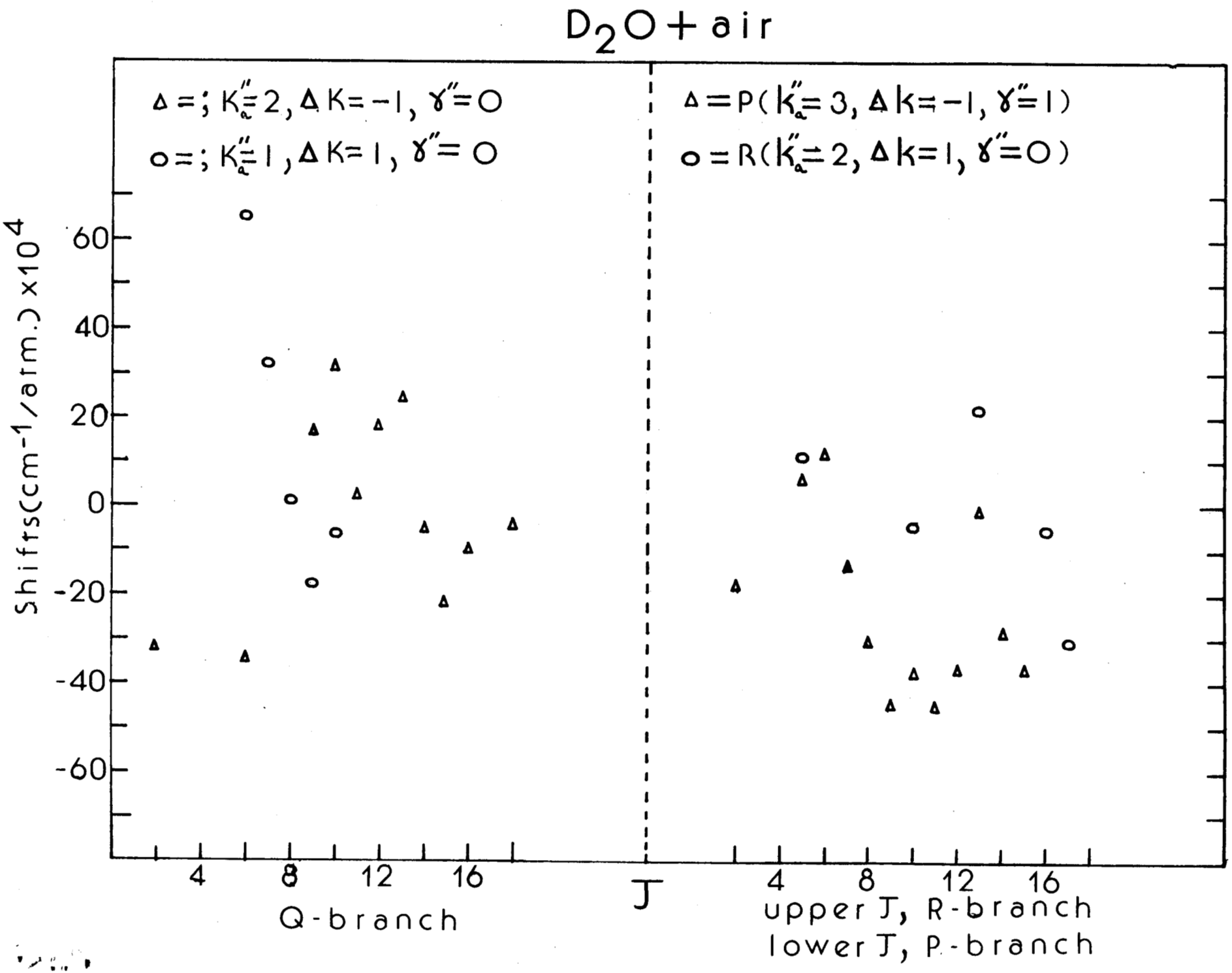
D_2O + air
Δ =; $K''_a = 2$, $\Delta K = -1$, $\gamma'' = 0$
o =; $K''_a = 1$, $\Delta K = 1$, $\gamma'' = 0$
Δ = P($K''_a = 3$, $\Delta k = -1$, $\gamma'' = 1$)
o = R($K''_a = 2$, $\Delta k = 1$, $\gamma'' = 0$)
Shifts(cm^{-1}/atm.) x10^4
60
40
20
0
-20
-40
-60
4
8
12
16
J
Q-branch
upper J, R-branch
lower J, P-branch